Akademie věd České republiky

Teze disertace k získání vědeckého titulu "doktor věd"
ve skupině chemických věd

Molecular structure of free boron and gallium clusters

Komise pro obhajoby doktorských disertací v oboru Anorganická chemie

Drahomír Hnyk

Ústav anorganické chemie AVČR, v.v.i.

Husinec - Řež, 2014

Jsem zavázán pracovníkům oddělení syntéz ÚACH AV ČR, v.v.i. za syntetický podtext mých strukturních studií. V tomto ohledu patří můj největší dík Dr. Josefu Holubovi za přípravu mnohých sloučenin „na míru“. Dnes již zesnulému Doc. Dr. Stanislavu Heřmánkovi vděčím za první kroky v borové chemii. Dr. Janu Macháčkovi vděčím za spolurealizaci některých výpočtů a technickou pomoc.

Děkuji Prof. Dr. Istvánu Hargittaiovi (Budapest) a Prof. Dr. Paul von Ragué Schleyerovi (dříve Erlangen, dnes Athens, GA, USA) za uvedení do problematiky elektronové difrakce resp. výpočetní chemie. Elektronově-difrakční studie by nikdy nebyly realizovány bez umožnění mých postdoktorálních pobytů u Prof. Dr. Davida W.H. Rankina v Edinburghu, za což též velmi vřele děkuji. Velmi oceňuji aktivní spolupráci s Prof. Dr. Michaelem Bühlem (St. Andrews) a Dr. Derekem Wannem (York, dříve Edinburgh), oba jmenovaní zaslouží též mimořádné poděkování.

Za pochopení strukturní chemie jako takové, zvláště pak za význam dipólových momentů v ní, vděčím svému nezapomenutelnému učiteli Prof. Dr. Otto Exnerovi. Děkuji Pane Profesore.

Děkuji též svým rodičům a dětem Míše, Lucce a Martinovi jakož i svým „sobotním“ přátelům, tito vždy dodávali mé práci lidský rozměr.

Bez účasti všech jmenovaných by tato práce nikdy nemohla vzniknout.

Říjen 2014 Drahomír Hnyk

To Josefina

Contents

Résumé

This thesis deals with gas-phase molecular structure determinations of neutral boranes and heteroboranes, as well as two examples of gallium clusters, employing the techniques of gas-phase electron diffraction (GED) and/or modern quantum chemical calculations. Such calculations were useful for computing various observables in order to facilitate the analysis of the electron diffraction data. Additionally, microwave spectroscopy was utilised for the two thiaboranes (in conjuction with the University of Oslo). Unless otherwise stated, the samples used for the work described throughout this thesis originated from the Institute of Inorganic Chemistry of the Academy of Science of the Czech Republic, v.v.i., while the GED studies were performed mainly in the School of Chemistry at the University of Edinburgh. The computational work was performed at the Computer-Chemie-Centrum of the University of Erlangen-Nürnberg and, later, at Edinburgh and Řež. The structurally characterised boron clusters belong to the range of structural motifs, from *closo* to *nido*, which obey Wade's rule.[†] Examples of boranes that do not obey Wade's rules were also studied, as were selected macropolyhedral clusters and metallaboranes. Finally, in order to gain an insight into electron density distribution, analyses of the experimental dipole moments were carried out for a few examples.

For the *closo* systems, both icosahedral and bicapped-square antiprismatic mono- and diheteroboranes were structurally investigated in the gas phase; such studies represent pioneering efforts in boron structural chemistry. As well as *exo*-substituted *o*-, *m*-, and *p*-carboranes (1,2-, 1,7-, and 1,12-$C_2B_{10}H_{12}$), unique icosahedral aza- and thiadodecaboranes were prepared and subsequently studied using GED. Compared to the structure of the parent *closo*-$B_{12}H_{12}^{2-}$, the pentagonal belts of B atoms adjacent to the heteroatoms were found to be expanded in size. In the case of *closo*-1-$NB_{11}H_{12}$, calculated ^{11}B NMR chemical shifts were used for the first time as an additional refinement condition during the least-squares refinements of the electron-diffraction data. The B_5 girdle was found to be less expanded than in the sulfur analogue, although the NB_5 pyramid appears to be flatter than the equivalent SB_5 unit in *closo*-1-$SB_{11}H_{11}$, which has also been studied using microwave spectroscopy and found to interact with two-dimensional aromatic molecules on the basis of so-called σ-holes. Bicapped-square antiprismatic *closo*-1-SB_9H_9 was also studied using GED and microwave

[†] Wade's (n+1) skeletal electron pair rule explains the electronic requirements for *closo*-deltahedral boranes and is the boron equivalent of Hückel's rule of organic chemistry, see also ref. 32.

spectroscopy. The structures determined show SB_4 pyramids with the expanded B_4 square bases. A dicarbaborane with similar geometry was also structurally characterised using GED. All of these experimental studies were supported by quantum-chemical calculations, which were also used for structural investigation of two phosphacarbaboranes with bicapped-square antiprismatic geometries.

Nido clusters were tackled to a lesser extent, with the main focus on various eleven-vertex tri- and tetraboranes with open pentagonal faces and icosahedral-like geometries where one vertex is missing in relation to a perfect icosahedron. Both electron diffraction and computations were performed for this series of compounds.

Structural studies of *arachno* systems were carried out for several boat-like and chair-like nine- and ten-vertex species, either by electron diffraction in conjuction with quantum chemistry or by purely computational efforts.

Two distinct geometries of B_4 clusters were studied representing both basket-type molecules and a tetrahedron cluster with four *t*-Bu groups attached to the four boron atoms; this latter structure does not comply with Wade's rules. Interestingly, GED showed its power in terms of an extremely small time scale in the latter study by deteriming torsional angles within *t*-Bu groups without needing to use any supporting data.

Whereas the earlier GED studies of boranes and carboranes ignored the calculated vibrational effects because of a lack of force fields for these clusters, the current electron diffraction investigations of boranes and various types of heteroboranes did use calculated force fields to good effect. They revealed an interesting feature: the amplitudes of vibration for bonded and nonbonded cage distances are very similar, which is at odds with various empirical rules suggesting that amplitudes of vibration should be roughly proportional to the corresponding internuclear distances.

One important aspect of boron cluster chemistry is the use of larger clusters in medicine, so far exemplified by various enzyme inhibitors. To this end a number of metallaboranes, as well as one macropolyhedral species, were studied computationally.

Gallium nitride represents one of the building blocks in microelectronics and is based on Ga_4 tetrahedral arrangement. Armed with this fact, two gallium clusters were also structurally studied using GED. They contain either sulfur or selenium atoms instead of nitrogen. The structures determined are based on two mutually fused tetrahedra. Again, torsional angles within *t*-Bu groups attached to four gallium atoms were unambiguously determined by electron diffraction alone. Such clusters are becoming important also in materials science.

Abbreviations

GED	Gas-phase Electron Diffraction
MW	Microwave Spectroscopy
MOCED	Molecular Orbital Constrained Electron Diffraction
SARACEN	Structure Analysis Restrained by *Ab initio* Calculations for Electron diffractioN
NMR	Nuclear Magnetic Resonance
IGLO	Individual Gauge Localised Orbitals
GIAO	Gauge Invariant Atomic Orbitals
DFT	Density Functional Theory
SCF	Self Consistent Field
MP2	Moller-Plesset Perturbation Theory of the Second Order
HF	Hartree-Fock Theory
B3LYP	Three-parameter stand alone hybrid functional of Becke
BP86	Exchange and correlation functional of Becke and Perdew
DZP	Double-zeta and polarization functions

Symbols

6-31G*	Pople's double-zeta basis set with one set of polarization functions
6-311G**	Pople's triple-zeta basis set with two sets of polarization functions
cc-pVTZ	Dunning's correlation consistent triple-zeta basis set
II	Huzinaga's triple-zeta basis sets
II'	Huzinaga's triple-zeta basis sets with double-zeta basis set on hydrogen atoms
AE1	combination of II' on main group elements and Wachter's basis sets on Ni
962(d)	Binning and Curtiss contraction of Dunning's primitive basis set on Se

C_x, D_y, T	the corresponding point group of symmetry (x = 1, 2, 2v, 4v, 5v, s; y = 2h, 2d, 5d)
τ	torsional angle

Colouring of atoms in the figures (based on Corey, Pauling and Koltun)

Hydrogen	blueish
Boron	green
Carbon	black
Nitrogen	skye blue
Sulfur	yellow
Fluorine, Chlorine	light green
Bromine	dark orange
Iodine	violet
Phosphorus	dark violet
Gallium	violet
Selenium	dark yellow
Nickel	orange

INTRODUCTION

Boron is one of only a few elements that is capable of forming extended binary hydrides. These so-called boranes do not occur in nature; rather they are exclusively products of man-made chemistry. Diborane, B_2H_6, can be considered as an archetype of boron hydrides; its structure was first reported in 1937 as being similar to that of ethane.[1] However, subsequent gas electron diffraction (GED) data were found to be incompatible with this ethane model, and the familiar D_{2h}-symmetric molecular geometry involving two bridging hydrogen atoms was introduced.[2] The bridging hydrogen atom is an essential structural motif for boron clusters and, together with BBB triangles, is observed for many boron hydrides and larger heteroboranes. The hydrogen bridge is an example of 3-centre-2-electron bonding, and this discovery led W. N. Lipscomb to formulate the concept of multicentre bonding, which resulted in the award of the Nobel Prize in 1976.

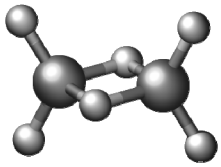

Diborane, B_2H_6

Borane architectures are based on three-dimensional structures composed of triangular B–B–B units. The immense variety of borane structures (stable, for example, as dianions, $B_nH_n^{2-}$) stems from the number of boron vertices, n (in the basic series n = 5-12), and the electrons available – thus we distinguish the closed-cage *closo*- species ($2n$ + 2 electrons) and several open-cage species, derived by notionally removing one (*nido*-, $2n$ + 4 electrons), two (*arachno-,* $2n$ + 6 electrons), or more *(hypho-,* $2n$ + 8 electrons*)* boron vertices. Due to the formal electron deficiency of boron atoms, their connectivity can be as high as six. The extreme stabilities of *closo* borane cages are due to the delocalisation of two surplus electrons of the dianions along the σ bonds of the whole cage.

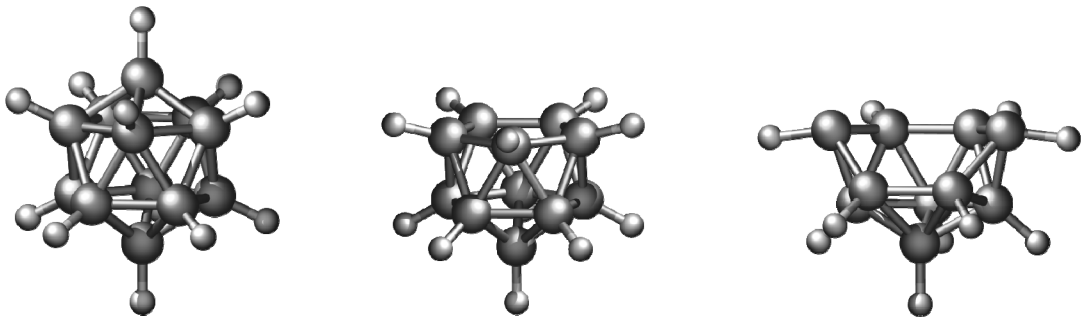

closo-$B_{12}H_{12}^{2-}$ *nido*-$B_{11}H_{11}^{4-}$ *arachno*-$B_{10}H_{10}^{6-}$

Schematic representation of the "*closo-nido-arachno*" relationship for deltahedral boranes

AIM OF THE DISSERTATION

Syntheses and molecular structure studies of boranes and heteroboranes at the Institute of Inorganic Chemistry of the Academy of Sciences of the Czech Republic, v.v.i. date back to the 1960s.[3] Elucidation of molecular structures, which can involve the determination of *molecular geometry*, *electron distribution*, and *intramolecular motion*, include both classical investigations in the solid state (by means of X-ray diffraction analysis) and those related to free molecules. The latter have been accomplished either using GED[4] or, more recently, using computational methods. Efforts are made to study isolated molecular structures because single crystals of many free heteroboranes are disordered and, consequently, determination of accurate structures in the solid state is impossible. It is these isolated-molecule geometries that are the subject of this dissertation aimed at expanding the body of knowledge of experimental geometries for free boranes and heteroboranes. There is an emphasis on generalising observed structural trends, including in relation to the unique gallium clusters studied, also with regard to the fact that both boron and gallium are significantly used in microelectronics.

METHODOLOGY

1. Determination of molecular structures

Electron diffraction is the most important technique for the determination of structures of gaseous molecules. GED is based on the scattering of a beam of higher-energy electrons from a gaseous sample of randomly orientated vibrating molecules. Significant contributions to the field were made in a number of laboratories, where the accelerating voltages for the

electrons were *ca.* 60 kV at Hungarian Academy of Sciences in Budapest, and *ca.* 42 kV at the Universities of Oslo and Edinburgh. Data for the vast majority of examples discussed here were collected at the School of Chemistry at the University of Edinburgh where I pursued my postdoctoral fellowships; any exceptions will be specifically mentioned in the text. Samples were typically heated to give sufficient vapour pressure, before the gas jet was intersected by the high-energy electron beam to yield one-dimensional diffraction patterns. After subtracting the scattering due to individual atoms, one is left with an experimental molecular scattering pattern from which the structure can be determined. The theoretical molecular intensity $M(s)$ (see Equation 1) comes from the theory of scattering and takes a geometrical model into account, which provides all interatomic distances, r_{ij} (Equation 1). Structural analysis is performed using a least-squares refinement procedure, fitting experimental and theoretical molecular intensities; the so-called R factor that is yielded is a mathematical measure of the fit of the model to the data.[5] It should be noted that the model describing the geometry of a molecule in terms of selected refinable geometrical parameters is an essential part of the analysis of electron-diffraction data, and that writing such a model with the minimum number of parameters possible is sometimes far from routine.[6]

$$M(s) = \alpha_{ij} \sum_{\substack{i=1 \\ i \neq j}}^{N} \sum_{j=1}^{N} g_{ij}(s) \cdot \exp\left(-\frac{1}{2} l_{ij}^2 s^2\right) \frac{\sin\left[s\left(r_a - \kappa_{ij} s^2\right)\right]}{s r_{ij}} \qquad (1)$$

The theoretical molecular intensity curve is a superposition of sinusoids for each atomic pair bounded by experimental limits of the scattering variable, s [= $(4\pi/\lambda)\sin(\theta/2)$], which is often reported in $Å^{-1}$. The meanings of other nonrefineable variables used in Equation 1 are as follows: λ is the electron wavelength, θ represents the scattering angle, and g_{ij} is supposed to be known in the structure analysis and is related to scattering factors and atomic phases. α_{ij} represents the weight of each distance and is related to conformational analysis since electron diffraction represents a particularly fast timescale (*cf.* 10^{-18} s compared to, for example, NMR for which the time scale amounts to 10^{-9} to 10^{-1} s). r_{ij} is the main result from the structural analysis and represents an effective internuclear distance; in other words it defines the *molecular geometry*. As well as geometric parameters, the GED refinements provide, in terms of vibrational amplitudes, l_{ij}, a good insight into relative vibrational displacements of the atomic nuclei with respect to their equilibrium positions. Initial values of vibrational amplitudes can either be calculated or estimated on the basis of data accumulated

for similar compounds. Hence, this method provides valuable pieces of information about *intramolecular motion*. Finally, κ_{ij} is an anharmonicity constant that is significant for bonded atom pairs and far less so for non-bonded pairs.

Sine Fourier transformation of this molecular scattering pattern gives rise to a radial distribution curve consisting of a peak for each interatomic distance in the molecule (Equation 2):

$$f(r) = \frac{2}{\pi} \int_0^{s_{max}} sM(s) \exp(-bs^2) \sin(sr)\, ds \qquad (2)$$

where $\exp(-bs^2)$ is an artificial damping factor introduced because the range of experimental data is reduced from $s = \langle 0, \infty \rangle$ to $s = \langle s_{min}, s_{max} \rangle$.

Analysis of electron-diffraction data is relatively easy for small, symmetrical clusters,[5] where it can provide very accurate results indeed. Conversely, larger, less symmetrical molecules (such as asymmetric boranes or heteroborane clusters) may be more demanding, and such investigations often necessitate the combination of electron-diffraction data with data obtained by other methods, both experimental and theoretical, in order to obtain reliable results.

The problems associated with refining the molecular structure of a borane or heteroborane using GED data alone stem from the fact that the molecules usually contain many atom pairs separated by the B–B bond length of around 170 to 190 pm. In general this can preclude the resolution of individual B–B distances with high accuracy because they are usually strongly correlated with one another. This inadequacy of GED can be overcome by supplementing the refinement with data obtained from geometry optimisations carried out at various levels of theory, and then fixing the differences between similar distances at computed values, *i.e.* as rigid constraints. This was known as the *MOCED* approach.[7] A superior approach, however, also utilising data from theoretical geometries, has been developed to allow the refinement of all geometrical parameters,[8] and it is the natural extension of *MOCED*. In essence this approach known as the *SARACEN* method hinges upon (a) the use of calculated parameters as flexible restraints (rather than rigid constraints), and (b) the refinement of all geometrical parameters as a matter of principle. The restraints are entered into the GED refinements as extra observations, just as is commonly done with

additional experimental data (*e.g.* rotational constants from microwave spectroscopy). More realistic estimated standard deviations are obtained as a consequence.

The architecture of a newly synthesised borane or heteroborane cluster is proposed on the basis of experimental measurements of the ^{11}B NMR spectrum (^{13}C NMR is also frequently applied in the case of carbaboranes), utilising various approaches, including decoupling and two-dimensional NMR techniques, such as COrrelated SpectroscopY. Chemical knowledge of related compounds is also considered. The chemical shifts obtained by such spectroscopic measurements are then defined relative to the usual standard of ^{11}B NMR spectroscopy, which is $BF_3{\cdot}OEt_2$.

Comparison of experimental and calculated ^{11}B NMR chemical shifts may also serve as a validation of the refined geometry, as the calculated shielding tensors are quite sensitive to small changes in the geometry of a cluster, with the hydrogen positions being particularly crucial. (Cartesian coordinates serve as the input for magnetic property calculations.) There may be several models that fit the GED data almost equally well, but not all of them provide calculated values of $\delta(^{11}B)$ that are in good accordance with experimental values. A number of borane and heteroborane geometries have been refined employing this joint *ab initio*/GED method,[D1] the final structures having been validated by Individual Gauge Localised Orbital (IGLO)[9] or Gauge Invariant Atomic Orbital (GIAO)[10] chemical shift calculations. These efforts will be exemplified below.

The *ab initio*/GIAO/NMR method, with DFT and IGLO variants, also provides the possibility of deriving internal coordinates for free boranes and heteroboranes, particularly for those that are negatively charged and/or possess no symmetry. The *ab initio*/GED method differs from this approach only by employing experimental geometries instead of theoretically derived ones. The dimensions of the proposed molecular shape are optimised by *ab initio* calculations, using Hartree-Fock theory to provide starting geometries for final computations that include the effects of electron correlation using, for example, the MP2 (Møller-Plesset second-order perturbation theory) method.[11] Density Functional Theory (DFT) methods also intrinsically involve correlation energy, but save both scratch disk space and memory as the corresponding orbitals are functions of just one variable, *i.e.* electron density, in contrast to the orbitals used for *ab initio* calculations which express the dependence on three variables, the *x*, *y*, and *z* coordinates for each atom of a cluster. The optimised geometry found in this way is then used as an input for the calculation of a shielding tensor, again employing IGLO- or GIAO-based methods. The GIAO-

MP2/II//MP2/6-31G*[‡] method for clusters containing just main-group elements (the most common are C, N, S, and P, with terminal hydrogens replaced by methyl, phenyl, or *t*-Bu groups) proved to be a very successful tool. The shielding tensor is calculated by the GIAO method at the MP2 level employing a TZP Huzinaga basis set[12] (denoted as II), utilising the molecular geometry derived with a Pople-style basis set of 6-31G*[13] and with the addition of MP2-type correlation energy. Larger systems demand more CPU and memory, but the GIAO-HF/II//MP2/6-31G* method gives spectral data that are quite sufficient for the purpose of confirming the correctness of a molecular structure. The latter approach differs from the former by not including the electron correlation for the magnetic property calculations, *i.e.* the SCF level is used.

The situation is more tricky for heteroboranes that contain a metal. The choice of basis set is important both for geometry optimisations (all-electron basis set *vs*. valence basis set with relativistic pseudopotentials) and for the evaluation of the shielding tensors, for which the computational method is also important. The most frequent approach, justified by some examples of successful applications, relies on the GIAO-DFT/basis set//DFT/basis set scheme, where the basis set is either all-electron or valence + pseudopotentials, and the DFT method is usually represented by the well-established functionals B3LYP[14] and BP86.[15] The calculated ^{11}B chemical shifts (with respect to $BF_3{\cdot}OEt_2$, diborane serving as a primary reference) are then compared with experimental ones. The level of agreement between computed and calculated spectra provides the basis for accepting or refusing a particular geometry, with a difference of 2 to 3 ppm (depending on the level of calculations) being considered acceptable. In cases where both experimental (GED) and theoretical geometries are available, ^{11}B chemical shift calculations allow the quality of the geometries to be assessed in terms of the agreement of the chemical shifts with the experimental data. Computed energies for such experimental structures may also be helpful; if one is much higher in energy (40 kJ mol^{-1} or more) than the optimised structure, then the experimental result is unlikely to be correct.

[‡] The nomenclature used to describe these calculations gives the method and basis set for the geometry optimisation after the //, while the method and basis set used to calculate the magnetic properties are stated before it.

2. Determination of electron distribution

Dipole moments were measured at 25 °C in benzene (usually five solutions, weight fraction 1.8×10^{-4} to 1.1×10^{-3}) using the method published by Guggenheim and Smith.[§] Relative permittivities were measured at 6 MHz on a home-made DK-meter with direct frequency reading. Refractive indices were measured on an Aerograph refractive index detector (Varian).

STRUCTURAL ANALYSES

A BORON CLUSTERS

The success of the earlier systematic application of the *ab initio*/IGLO/NMR method and its GIAO variant for the structural studies of carbocations[16] has led to the application of the method to boranes and heteroboranes, with the common characteristic of electron deficiency in carbocations and boranes and heteroboranes providing the driving force for this extension. Beaudet[17] has reviewed structures of small and medium-sized boranes and carbaboranes, determined by GED, X-ray diffraction, and microwave spectroscopy, and the validity of the structures was later checked using the *ab initio*/IGLO/NMR method.[18] As for reviewing gas-phase structures of parent and *exo*-substituted boranes and carboranes of larger dimensions (n = 10, 12), it was Mastryukov who did this work.[19] However, he successfully attempted to review only molecular structures that were determined by GED alone. The gas-phase structures of two heterocarboranes, *viz. closo*-1,12-$CHXB_{10}H_{10}$ (X = P, As) also appeared in the latter review. To my knowledge, there were no gas-phase structures of heteroboranes apart from the carboranes and two heterocarboranes, as confirmed by refs. 18-20. Here I aim to summarise molecular structures of both older and newly prepared neutral boranes and heteroboranes determined by using GED and/or modern computational protocols. Unless otherwise stated, all the compounds presented were prepared at the Institute of Inorganic Chemistry of the ASCR, v.v.i. Additionally, I also tackled two gallium clusters to see whether there is a relationship between structural chemistries of boron and gallium.

[§]It is pertinent to recall that measurements of electric dipole moments are based on the Debye equation. The third term of it, the orientation polarization P_O, is the essence of most experimental procedures to determine dipole moment. See e.g. O. Exner, Dipole Moments in Organic Chemistry, Georg Thieme Publishers, Stuttgart, 1975.

1. Parent boron hydrides

Pentaborane(11), *arachno*-B_5H_{11} (**1a**), was prepared at the University of Leeds and was the first small borane to which the *ab initio*/IGLO/NMR method was applied (Figure 1).[20] This study revealed that the structure in which the apical bridging hydrogen is involved in a rather ordinary three-centre hydrogen-bridge bond, with the molecule having C_1 symmetry, is superior to that in which this hydrogen atom bridges three boron atoms at the same time (C_s symmetry), as had been proposed in an earlier analysis of GED data.[21] There was a remarkably good fit between the calculated (DZ//MP2/6-31G*) and experimental ^{11}B values for the C_1 structure, with a maximum deviation of *ca.* 3 ppm, whereas large discrepancies, up to *ca.* 8 ppm, were found for the original GED-based C_s structure.[21] In this preliminary GED study B_5H_{11} was constrained to have overall C_s symmetry. However, when this was relaxed in the *ab initio* (MP2/6-31G*) optimisation it was revealed that, for example, the B(2)–B(3) and B(4)–B(5) distances (assumed to be equal in the original GED refinement) differed considerably, at 173.7 and 181.0 pm, respectively.

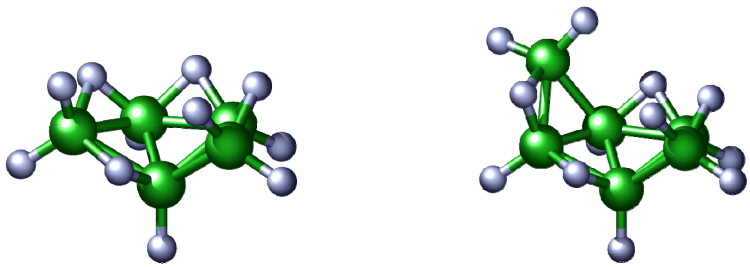

1a **1b**

Fig. 1 *Arachno* boranes B_5H_{11} and B_6H_{12}

Although both the GED[22] and *ab initio* geometries[23] for another small borane (also prepared at Leeds), hexaborane(12), *arachno*-B_6H_{12} (**1b**), demonstrated C_2 symmetry and the same pattern of bridging hydrogen atoms, the derived structural parameters differed even more noticeably than for B_5H_{11} (Figure 1). For example, the assumption that the B(1)–B(6) nearest-neighbour separation is greater than B(1)–B(2) in the GED analysis was far from true in the results of the MP2/6-31G* calculations[23] [191.3 and 177.8 pm *vs.* 172.8 and 189.9 pm for the B(1)–B(6) and B(1)–B(2) separations, respectively]. It should also be noted that the single-point MP2/6-31G* energies calculated using the GED geometries for both molecules

were much higher than those optimised at the MP2/6-31G* level[20,23] especially for B_6H_{12} (247 kJ mol^{-1}).

Given the NMR and energetic evidence that the original GED structures might not be correct, the electron-diffraction data for **1a** and **1b** were reanalysed. The new models for both B_5H_{11} and B_6H_{12} considered the theoretical geometries, but inspection of the resulting parameters for the original GED geometries revealed that some vibrational amplitudes might not be correct. Such amplitudes might be expected to have similar values for all the nearest-neighbour separations, and similarly for all the next-nearest (or for the next-next-nearest) neighbour separations. In the refinements these vibrational terms were refined in groups, with little variation between members of any one group, while C_1 and C_2 symmetries were chosen for **1a** and **1b**, respectively, with differences between related bond lengths fixed at values obtained in the MP2/6-31G* calculations. These refinements yielded new optimum geometries with improved *R* factors for both molecules,[D2] and both energetic and NMR criteria indicated that the new structures were much more satisfactory. For hexaborane(12) the excess energy of the experimental structure dropped from 247 to 47 kJ mol^{-1}, and the maximum deviations between the DZ//new-GED calculated and experimental ^{11}B chemical shifts were reduced to around 3 ppm. The agreement for **1a** was actually better than that for the computed (DZ//MP2/6-31G*) and the experimental values. The refined vibrational amplitudes in **1b** were also much more realistic; for example, those for B(1)–B(2) and B(1)···B(5) now refined to 7.2(2) and 7.9(4) pm, respectively.

2. *Closo* heteroboranes

a) Icosahedral dodecaborane(12) derivatives

The idea that amplitudes of vibration of both closely-spaced atomic pairs and those more widely separated might have similar values in *arachno* systems has been prompted by the determination of the molecular structure of a member of another family of boron clusters known as *closo* systems, *i.e.* 1-thia-*closo*-dodecaborane(11), *closo*-1-$SB_{11}H_{11}$ (**2a**) (ref. D3) for which the electron-diffraction data were recorded in Budapest. A model assuming C_{5v} symmetry led to a distortion from a regular icosahedral structure, consisting mainly of a substantial expansion of the pentagonal belt adjacent to sulfur (Figure 3). The B–B distances in this pentagon refined to 190.5(4) pm, the other B–B distances all falling in the narrow range from 177.7 to 178.3 pm. The S–B bond is the longest in the molecule, 201.0(5) pm.

Amplitudes of vibration are consistent with those found for **1** and **2**, *e.g.* 5.1(4) and 6.8(3) pm for B(2)–B(3) and B(2)···B(9), respectively. The latter value is smaller than that for S–B(2), 7.1(4) pm, even though the two atoms are on opposite (rather than adjacent sides) of the molecule. This strongly supports the idea that a *closo* structure is particularly rigid. Even the HF/3-21G* and HF/6-31G* (ref. 24) parameters agree quite well with the experimental findings [*e.g.* B(2)–B(3) at HF/6-31G* is 190.4 pm, just 0.1 pm from the experimental value]. This observation is also reflected in very good agreement between the DZ//GED and DZ//HF/(both basis sets) ^{11}B chemical shifts; both computed sets of shifts also compared well with the corresponding measured values.

Geometry optimisations for **2a** have been performed at higher levels of theory in another context. DFT calculations at the B3LYP/cc-pVTZ level were undertaken to see the effect of this computational protocol on the molecular geometry. [S–B and B(2)–B(3) optimised to 202.0 and 189.0 pm.] This work also reported the results of an investigation of the structure of **2a** by microwave spectroscopy[D4] but positions of hydrogens were experimentally located only by GED investigation.[D3] This microwave study resulted in a precise substitution structure for the non-hydrogen atoms, with S–B at 201.3(2) pm and B(2)–B(3) at 188.9(1) pm. The MP2/6-31G* geometry of **2a** has also become available, along with those for some 12-X derivatives[D5] (X = F, Cl, Br, and I, **2b**, **2c, 2d**, and **2e**, respectively, Figure 2). However, instead of the 6-31G* basis set used for X = H (**2a**), F (**2b**) and Cl (**2c**),

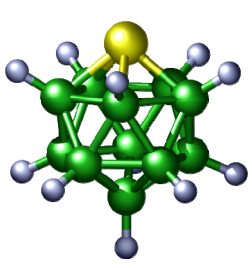

2a

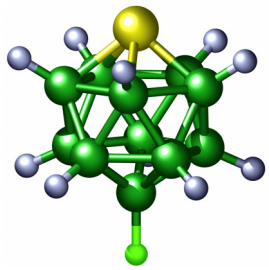

2b

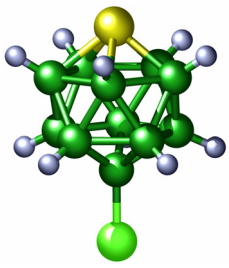

2c

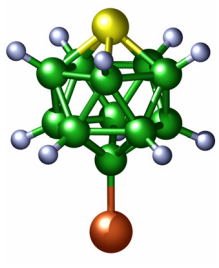

2d

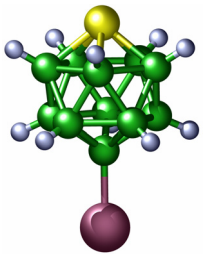

2e

Fig. 2 *Closo*-1-$SB_{11}H_{11}$ and its halogen derivatives

quasi-relativistic energy-consistent pseudopotentials[25] with DZP valence basis sets were employed for X = Br (**2d**) and I (**2e**). The S–B and B(2)–B(3) separations in **3a** at the MP2/6-31G* level converged to 200.0 and 187.6 pm, respectively. It is apparent that the nearest-neighbour BB separations computed at the HF level were overestimated in relation to those derived at the correlated MP2 level of theory (and DFT). As noted earlier, errors of 5 to 10% are possible, depending on the theory used.[18] Halogen substitution does not have any significant influence on the overall geometry of the icosahedral cage. A change in the chemical shift of B(12), the so-called antipodal chemical shift,[D6,D7] is reproduced quite well at GIAO/II//MP2/6-31G* for **2a** and **2c** and also by including spin-orbit corrections[26] for **2d** and **2e**. Dipole moments of **2a**, **2c**, **2d** and **2e** that were measured and published in ref. D5 showed without doubt that the sulfur atom is positively charged.

The structure of the selenium analogue of **2a**, *closo*-1-$SeB_{11}H_{11}$, **3** (Figure 3a), has also been determined using the *SARACEN* method,[D8] and this work provided an unambiguously determined Se–B bond length without using any restraint. This finding can be used in terms of testing the quality of various computational protocols. For **3**, as was also the case for 1-$SB_{11}H_{11}$, *ab initio* geometries slightly underestimate the expansion of the pentagonal belt adjacent to the chalcogen, the centre of positive charge of the cluster. For example, MP2/962(d) gives 190.9 pm for this B–B distance, compared with 192.2(2) pm as determined by GED alone.

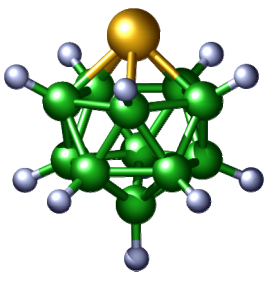

a

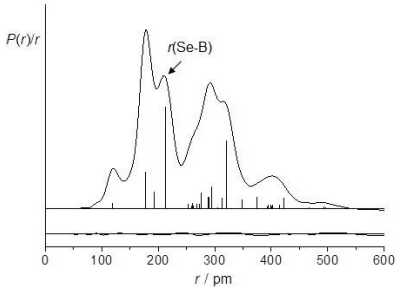

b

Fig. 3 *Closo*-1-$SeB_{11}H_{11}$: **a** molecular structure, **b** radial distribution curve

There are other main-group elements that can replace $(BH)^{2-}$ vertices of the I_h-symmetric (*closo*-$B_{12}H_{12})^{2-}$. Just as S is isoelectronic with $(BH)^{2-}$ so, for example, is $(CH)^-$, which plays the same role. Replacement of one $(BH)^{2-}$ vertex in *closo*-$B_{12}H_{12}^{2-}$ will thus lead to (*closo*-1-$CB_{11}H_{12})^-$. The MP2/6-31G* calculated structure has been reported as well as solid-state structures with various cations.[27] In contrast, if two $(BH)^{2-}$ groups in the parent dianion are replaced by two $(CH)^-$ moieties, three isomeric twelve-vertex neutral dicarbaboranes can be obtained, *i.e.* *closo*-1,2-$C_2B_{10}H_{12}$, *ortho*-carbaborane, **4a** (C_{2v} symmetry), *closo*-1,7-$C_2B_{10}H_{12}$, *meta*-carbaborane, **4b** (C_{2v} symmetry), and *closo*-1,12-$C_2B_{10}H_{12}$, *para*-carbaborane, **4c** (D_{5d} symmetry). They are ideal targets for gas-phase electron diffraction.[28]

Structures of molecules derived from all three parent icosahedral carbaboranes by substitution of terminal hydrogen atoms on carbon have also been determined by the combined use of GED and *ab initio* calculations. These include 1-Ph-1,2-dicarba-*closo*-dodecaborane(12), 1-Ph-1,2-*closo*-$C_2B_{10}H_{11}$, **4a1** (prepared at the University of Edinburgh),[D9] 1,2-dicarba-*closo*-$C_2B_{10}H_{10}$-9,12-dithiol, 9,12-$(SH)_2$-*closo*-1,2-$C_2B_{10}H_{10}$, **4a2**,[D10] 1,7-dichloro-1,7-dicarba-*closo*-$C_2B_{10}H_{10}$, 1,7-Cl_2-1,7-*closo*-$C_2B_{10}H_{10}$, **4b1**,[D11] and 1,12-dicarba-*closo*-$C_2B_{10}H_{10}$-1,12-dithiol, 1,12-$(SH)_2$-*closo*-1,12-$C_2B_{10}H_{10}$, **4c1**[D12] (Figure 4). The effect of the phenyl substituent on the C–C bond length in **4a1**, 162.7(8) pm compared with 162.4(8) pm in its parent **4a**, is marginal. This parameter in **4a1** can probably be considered to be determined accurately, because the *SARACEN* method was used, in this case for the first time in the determination of the molecular structure of a borane or heteroborane. This observation strongly indicates that there is no conjugation between the two-dimensional and three-dimensional moieties comprising **4a1**. Indeed, a dipole moment study of **4a** indicates that it behaves as a slight electron acceptor only.[D13] Using a vector solution of a triangle within this study unambiguously revealed that the midpoint of the CC

vector is the centre of positive charge with a dipole moment of 4.50 D. The molecule has overall C_1 symmetry, in which the C_6 hexagon eclipses the C(1)–B(4) bond. IGLO/II′//GED and IGLO/II′//HF/6-31G* calculations (II′ is the same TZP basis set as II but DZ is employed for hydrogens) support this finding. Similarly, the presence of two chlorines do not bring about any significant changes to C–B and B–B nearest-neighbour separations in **4b1** with respect to **4b**, C_{5v} symmetry for the CB_5 pentagonal pyramids in **4b1** having been assumed. Again, IGLO/II′//GED and IGLO/II′//MP2/6-31G* values agree well with one another, and with the experimentally determined $\delta(^{11}B)$ values. Thus the evidence strongly supports the accuracy of the experimentally and theoretically determined geometries.

Because the electron-scattering ability of sulfur is greater than those of hydrogen and carbon (the corresponding radial distribution curve are indeed richer in structural information), the cage geometries of 9,12-$(SH)_2$-*closo*-1,2-$C_2B_{10}H_{10}$, **4a2**, and 1,12-$(SH)_2$-*closo*-1,12-$C_2B_{10}H_{10}$, **4c1**, should be determined more accurately than the geometries of **4a** and **4c**, respectively, without the need for many constraints or restraints from theoretical calculations. The molecule have overall C_1 and C_2 symmetries, respectively, but local C_{2v} and D_{5d} symmetries for the carbaborane core were assumed, as this was shown to be appropriate within very close limits by calculations at the MP2 levels. As for **4a1** and **4b1**, the C–B and B–B distances in **4a2** and **4c1** were found to be unaffected by the substitutions at the carbon atoms. Armed with the results for a series of *p*-disubstituted benzenes,[27] I tested the possible influence of various substituents on the body diagonal, C(1)···C(12), of **4c**. The structures of a series of 1,12-X_2-*closo*-1,12-$C_2B_{10}H_{10}$ molecules[D12] were optimised (X = H, Li, BeH, BH_2, Me, SiH_3, NH_2, OH and F, as well as SH). This distance ranges from 303.1 pm for F to 317.1 pm for Li, *i.e.* the influence of electronegativity is appreciable. The same trend has been noticed for B(2)–C(1)–C(12) bond angles, twice the B(2)–C(1)–C(12) angle (126.0° for F and 122.0° for Li) being viewed as an analogue of the *ipso* angle in *para*-disubstituted benzene derivatives. A dipole moment study of 1,12-substituted derivatives of **4c** showed, as was the case for **4a**, a slight electron-acceptor ability of **4c**.[D14] When a *p*-carborane cage is substituted using a *p*-substituted phenyl group (4-X-C_6H_5), the cage acts as a very weak π-acceptor toward the phenyl if X represents an uncharged group.[**]

[**] A. R. Campanelli, A. Domenicano and D. Hnyk, *J. Phys. Chem. A*, submitted for publication, 10, 2014.

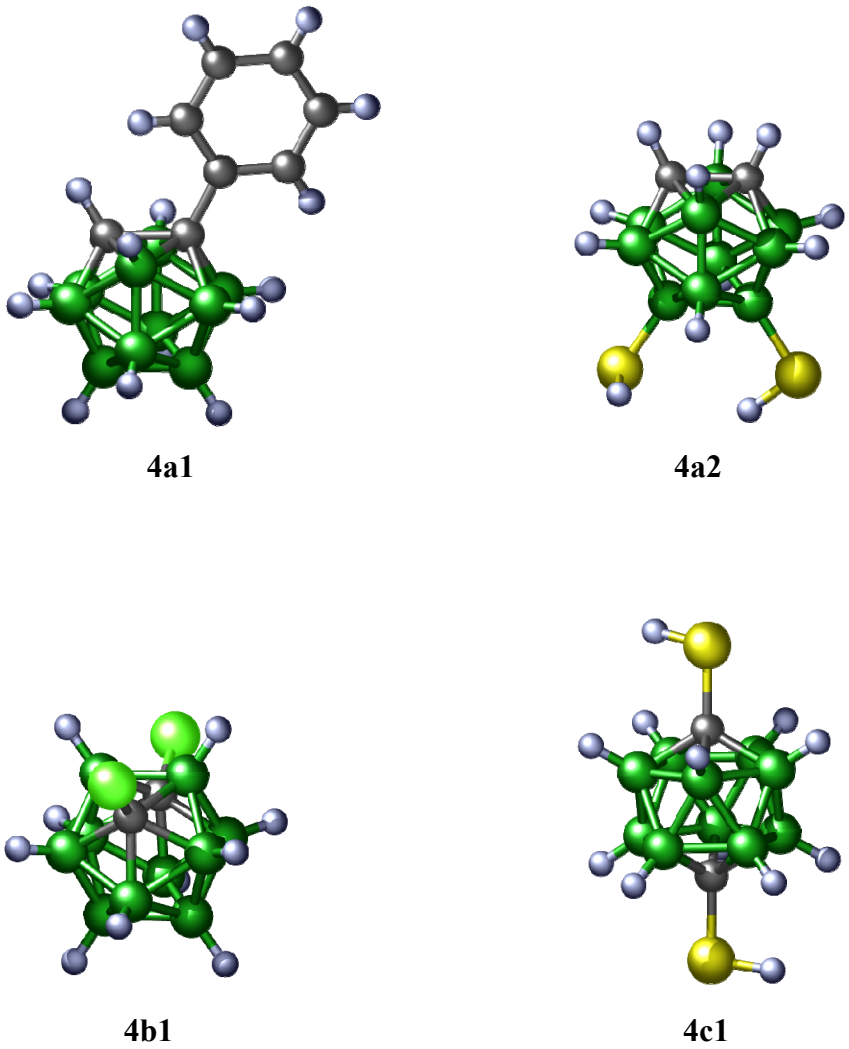

Fig. 4 *Closo*-$C_2B_{10}H_{12}$ derivatives

Continuing along the first row of the periodic table, NH is also isoelectronic with $(BH)^{2-}$, and the structure of another compound formally related to (*closo*-$B_{12}H_{12})^{2-}$, 1-aza-*closo*-dodecaborane(12), *closo*-1-$NB_{11}H_{12}$, **5**, (Figure 5), has been determined by a combination of computational methods and GED (provided by the University of Aachen and data recorded at the University of Oslo).[D1]

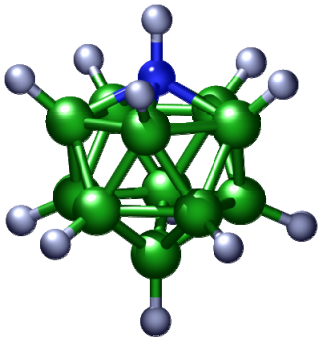

5

Fig. 5 *Closo*-1-$NB_{11}H_{12}$

Because the nitrogen atom is so much smaller than the sulfur atom in **2a**, the BN and BB distances calculated *ab initio* lie within a relatively small range of *ca*. 10 pm, which makes the structure determination from GED data much more difficult. In fact, four models with C_{5v} symmetry fit the data almost equally well. The ^{11}B NMR chemical shifts have been used to decide which of these possibilities is the most reasonable. The final experimental geometry was selected on the basis of the best agreement between the IGLO/DZ//GED and experimental ^{11}B chemical shifts. This was the first time that this method had been employed as an additional refinement condition in conjunction with GED structure determination. The single-point calculations at the MP2/6-31G* level supported this observation. The elongation of the B(2)–B(3) bonds in **5** [182.5(6) pm] is less than in **2a**, and the NB_5 pentagonal pyramid is flattened as a consequence of the short B–N bond [171.6(9) pm]. All of these differences can be attributed to the smaller size of the nitrogen substituent relative to sulfur.

It is also possible for bare phosphorus atoms to replace $(BH)^{2-}$ vertices in (*closo*-$B_{12}H_{12})^{2-}$. Substituted species that have been prepared include 1,2-diphospha-*closo*-dodecaborane(10), *closo*-1,2-$P_2B_{10}H_{10}$, **6a**, a few of its monochloro and dichloro derivatives such as 3-Cl, 4-Cl, 3,6-Cl_2 and 3,4-Cl_2 compounds, 1,7-diphospha-*closo*-dodecaborane(10), *closo*-1,7-$P_2B_{10}H_{10}$, **6b**, (Figure 6). The hypothetical 1,12-diphospha-*closo*-odecaborane(10), *closo*-1,12-$P_2B_{10}H_{10}$ was also computationally studied.

6a **6b**

Fig. 6 *Closo*-$P_2B_{10}H_{10}$ isomers

The structures of all of these icosahedral cages have been determined by an *ab initio*/GIAO/NMR method, *viz.* GIAO-HF/II//MP2/6-31G*.[D15] The presence of phosphorus at two vertices in **6a** and **6b** causes considerable distortions of the parent icosahedral skeleton (*closo*-1,12-$P_2B_{10}H_{10}$ being distorted along its body diagonal). For example, the B(3)–P(2)–B(6) and B(8)–P(7)–B(11) angles are reduced from the ideal 108.0° to 93.0° and 93.5°, reflecting the large size of the phosphorus atoms, which, like sulfur, have long bonds to their neighbouring boron atoms. As in the preceding cases, the very good agreement between the computed and experimental ^{11}B NMR chemical shifts indicates that the geometries of **6a** with its monochloro and dichloro derivatives and **6b**, calculated at the MP2/6-31G* level, may be accepted as reliable representations of their solution-state structures.

b) Bicapped-square antiprismatic decaborane(10) derivatives

The bicapped-square antiprismatic arrangement is known to be the basic building block for ten-vertex *closo* systems. The parent compound is represented by (*closo*-$B_{10}H_{10}$)$^{2-}$, which adopts D_{4d} symmetry. Again, by replacing $(BH)^{2-}$ vertices (although that is not as simple in the synthetic route) a number of ten-vertex *closo* species can be formed. As with **2a**, incorporation of sulfur leads to a *closo*-thiaborane, 1-thia-*closo*-decaborane(9), *closo*-1-SB_9H_9 (**7**), Figure 7 (C_{4v} symmetry).

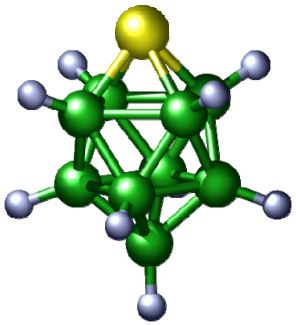

7

Fig. 7 *Closo*-1-SB_9H_9

There have been two studies dedicated to the molecular structure of **7**. First, the microwave spectrum of **7** was investigated[D16] and, as with **2a**, a precise substitution structure of the non-hydrogen atoms was determined. The most striking feature was a substantial expansion of the boron square adjoining sulfur, with *r*[B(2)–B(3)] = 193.7(1) pm, slightly longer than in **2a**. Supplementary high-level *ab initio* (MP2/6-311G**) and DFT calculations (B3LYP/6-311G** and B3LYP/cc-pVTZ) have confirmed this result. GED data have also been collected, and the *SARACEN* method has been applied,[D17] with results consistent with those obtained by theory and by rotational spectroscopy. The theoretical and GED geometries have been used for magnetic property calculations, but the MW geometry was not used, because the hydrogen-atom positions had not been determined. The three GIAO-HF and GIAO-MP2 sets of $\delta(^{11}B)$ values are in good agreement with experiment, but the latter approach is superior to the former in accounting for the chemical shift of B(10) which has the value 74.5 ppm (the difference from GIAO-MP2 is up to 1 ppm, depending on the geometry used). This is one of the most extreme ^{11}B chemical shifts to high frequency, this atom being antipodally coupled with sulfur, in a similar manner to the B(12)···S couple in **2a**, in which such a chemical shift is measured to be 18.4 ppm in $CHCl_3$. Such a difference of almost 60 ppm is accounted for by the occurrence of paramagnetic contributions to the magnetic shielding constants. These contributions arise from the coupling of suitable occupied and unoccupied molecular orbitals with large coefficients on B(10) and B(12), respectively, the latter being more pronounced in the case of ten-vertex thiaborane.

As in the case of $(B_{12}H_{12})^{2-}$, one $(BH)^{2-}$ vertex can be formally replaced by an isoelectronic $(CH)^-$ unit, resulting in $(closo\text{-}1\text{-}CB_9H_{10})^-$,[30] while substitution at two $(BH)^{2-}$ vertices provides three isomeric *closo* ten-vertex dicarbaboranes: *closo*-1,2-$C_2B_8H_{10}$, *closo*-

1,6-$C_2B_8H_{10}$, and *closo*-1,10-$C_2B_8H_{10}$. Whereas the structure of the last molecule has been determined by GED alone,[31] we have examined the first isomer, 1,2-dicarba-*closo*-decaborane(10) (**8**), (Figure 8) by the joint *ab initio*/IGLO/GED method.[D18]

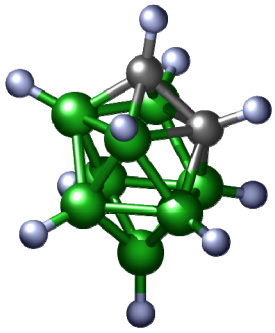

8

Fig. 8 *Closo*-1,2-$C_2B_8H_{10}$

In this case the electron-diffraction data were analysed using the *MOCED* approach. This molecule has C_s symmetry only, and conversion of the molecular scattering intensity to the radial distribution curve indicated that the data were very poor in structural information. Using GED data alone would have not given a realistic chance of determining the structure, and so the differences between similar bond lengths were fixed at the values calculated at the MP2/6-31G* level. The C–C bond length refined to a typical "alkane" value of 153.8(8) pm and leads to distortion from the regular bicapped-square antiprismatic shape. The displacement of the carbon atom towards the centre of the cluster results in a substantial opening of the B(3)C(2)B(5) bond angle, to 95° from the parent 90°. IGLO/DZ calculations have confirmed the reliability of both the experimental and theoretical (MP2/6-31G*) geometries.

As in the twelve-vertex *closo* system, phosphorus can also occupy positions in the bicapped-square antiprismatic skeleton. Two isomeric ten-vertex *closo* phosphaboranes, 2,1- and 6,1-*closo*-PCB_8H_9, **9a** and **9b**, respectively (both C_s symmetry, Figure 9), have been prepared.[D19] As in **8**, phosphorus atoms are pushed away from the centre of the cluster relative to the positions that they would adopt in a regular bicapped-square antiprism, and so the B(3)P(2)B(5) and B(7)P(6)B(9) angles in **9a** and **9b**, respectively, are narrowed by *ca*. 13° from the 90° expected in the regular polyhedron.

9a **9b**

Fig. 9 *Closo*-CPB_8H_9 isomers

3. *Nido* heteroboranes

By removing one BH vertex from a closo system, a *nido* skeleton is formally derived. As with the *closo* family, $(BH)^{2-}$ vertices can be replaced by heteroatom-based moieties, such as $(CH)^{-}$, S, NH, and P. We have been able to elucidate the structure of such a *nido* skeleton for the first time by using the joint *ab initio*/GED approach (data recorded in Oslo), using the *MOCED* method. The compound studied, 7,8-dicarba-10-thia-*nido*-undecaborane(10), 7,8,10-$C_2SB_8H_{10}$, **10**, (Figure 10),[D20] adopts C_s symmetry.

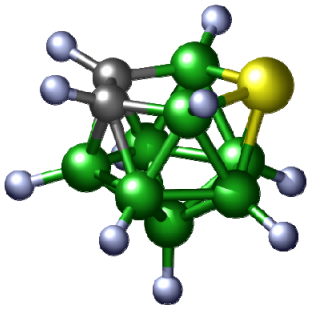

10

Fig. 10 7,8,10-*nido*-$C_2SB_8H_{10}$

Distortion of the C(7)C(8)B(9)S(10)B(11) open pentagonal ring is quite pronounced. For example, the B(9)S(10)B(11) angle is very narrow [GED: 93.1(6)°, MP2/6-31G*: 96.6°] compared to the 108.0° of a regular pentagonal ring. As a consequence, the sulfur atom lies

slightly out of the plane of the open pentagonal ring that exists in the hypothetical (*nido*-$B_{11}H_{11}$)$^{4-}$. IGLO/DZ calculations performed with both the GED and MP2/6-31G* geometries confirm the high quality of both of them.

There are also neutral compounds with substituents for boron at four vertices in the parent B_5 open pentagon, with two carbon and two phosphorus atoms, *i.e. nido*-$P_2C_2B_7H_9$ in the form of 7,8,9,11- (**11a**), 7,9,8,10- (**11b**) and 7,8,9,10- (**11c**) isomers (Figure 11). The last possible isomer, 7,10,8,9-, has so far only been examined computationally, because its energy is the highest of the four C_2P_2 isomers, and it has not yet been accessible experimentally.[D21] As expected, the presence of two phosphorus atoms leads to significant distortion of the five-atom ring, and the bond angles within it are either around 115° or around 96°. Some dihedral angles within these B_5 rings are as high as 20 to 28°.

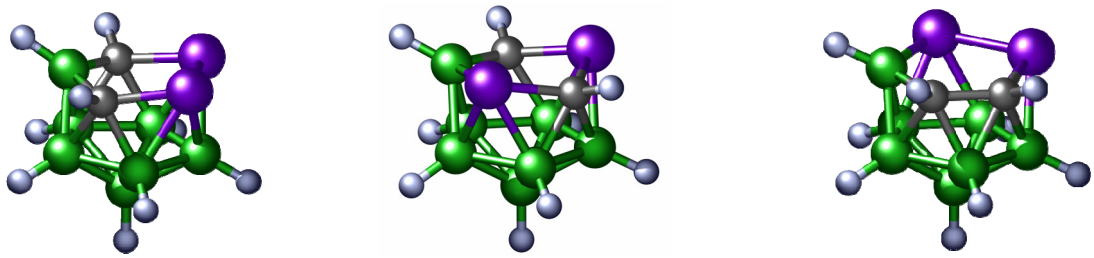

11a **11b** **11c**

Fig. 11 Tetrahetero analogues of 7,8,10-*nido*-$C_2SB_8H_{10}$

4. *Arachno* heteroboranes

Arachno compounds are formally derived from *nido* ones in the same manner as *nido* structures are from *closo*, that is by removing one BH vertex from the *nido* skeleton. For example, the hypothetical *nido*-$B_{11}H_{11}^{4-}$ yields the hypothetical *arachno*-$B_{10}H_{10}^{6-}$. The latter should exhibit a hexagonal boat-like shape, which is present in *arachno*-6,9-$C_2B_8H_{14}$, **12a**[D22] and *arachno*-6,9-CSB_8H_{12} **12b**,[D23] studied using the *SARACEN* method. Computational studies have also been performed for some analogues of **12a** and **12b**, *i.e. arachno*-6,9-$N_2B_8H_{12}$,[D22] **12c**, *arachno*-6,9-$Se_2B_8H_{10}$,[D22] **12d**, and *arachno*-6,9-CNB_8H_{13}, **12e**[D23] (Figure 22). The presence of heavy atoms (S, Se) brings about a considerable narrowing of the B–S(Se)–B angles. On the other hand, short N–B distances are responsible for flattening **12c** and part of **12e** with respect to (*arachno*-$B_{10}H_{14}$)$^{2-}$.

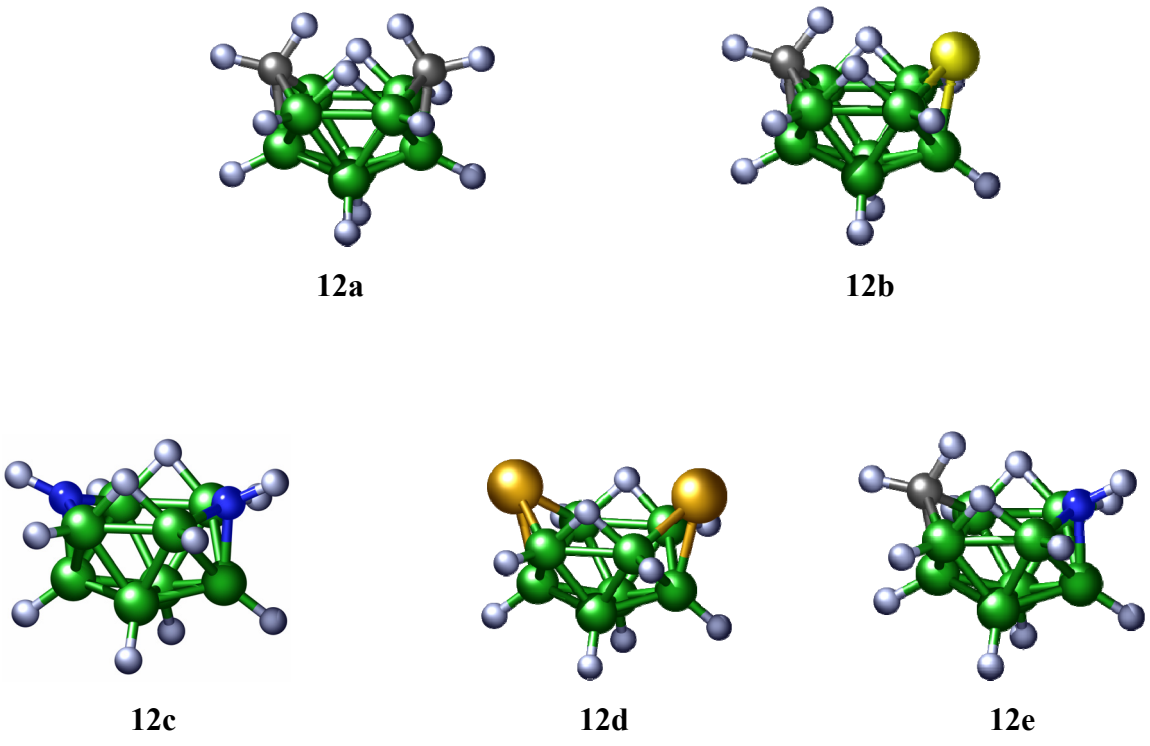

Fig. 12 Various *arachno* boat-like structures

Apart from ten-vertex *arachno* molecules, there are structurally characterised *arachno* systems of smaller dimensions as exemplified by *arachno*-4,6-$C_2B_7H_{13}$, **13a**,[D24] *arachno*-4,6-$S_2B_7H_9$, **13b**,[D24] and *arachno*-4,6,5-$C_2SB_6H_{10}$, **13c**.[D25] Their structures (C_s symmetry) have been elucidated by the *SARACEN* method (**13a**, **13b**) and using the *ab initio*/IGLO/NMR (**13c**) method.

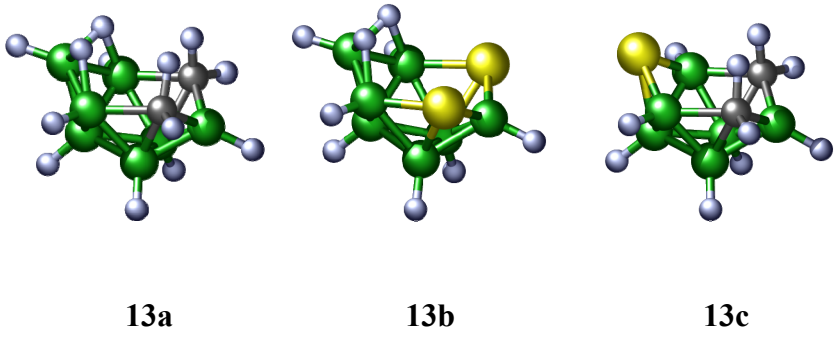

Fig. 13 Nine-vertex *arachno* structures

The derivation of the GED model for **13a** follows essentially the same route by which it was synthesised, involving the removal of three BH vertices from **4b**. In essence, the molecular shapes of **13a-13c** stem from the preceding family of *arachno* heteroboranes with one vertex missing.

5. B_4 clusters

Tetraborane(10), *arachno*-B_4H_{10}, was reacted at the University of Leeds with ethene to produce the so-called 2,4-ethanotetraborane(10), 2,4-$CH_2CH_2B_4H_8$,[D26] **14a** (Figure 14), in which the "wing" boron atoms of the "butterfly-shaped" B_4H_8 unit are attached to the C_2H_4 moiety. This structure with C_{2v} symmetry has been determined by the *MOCED* approach and both GED and MP2/6-31G* geometries have been verified by IGLO ^{11}B chemical shifts. The C–C bond length is 155.4 pm as obtained from MP2/6-31G* optimisations, and 156.8 pm in the GED experiment, although this parameter was fixed in the final GED refinement. The value is towards the long end of the range exhibited by alkanes. The *SARACEN* approach has also been applied to determine the structure of 2,4-(*t*-butylethano)tetraborane(10), 2,4-(*t*-BuCHCH$_2$)B_4H_8, **14b** (Figure 14, provided by the University of Leeds).[D27] The effect of the *t*-Bu group is quite marked, as the C–C bond of the C_2B_4 core is twisted by 6.6(14)°. As a consequence, the local symmetry of the C_2B_4 moiety is reduced from C_{2v} to C_2, the concomitant distortion of the B_4H_8 group from C_{2v} local symmetry being negligible.

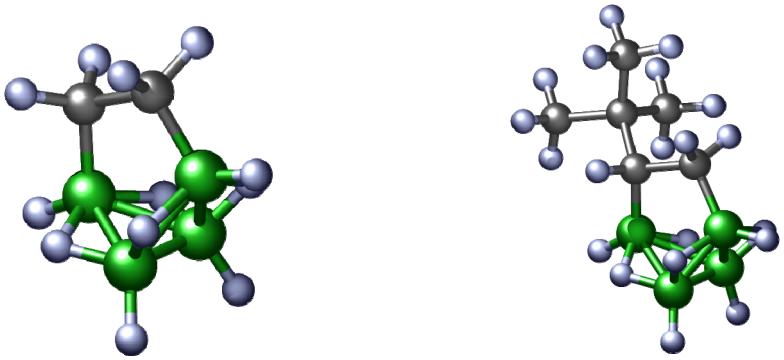

14a **14b**

Fig. 14 Ethano tetraboranes

In addition to the clusters complying with the rule that $n + 1$ electron pairs are optimal for n-deltahedral framework bonding,[32] there are boron clusters that represent exceptions to this rule. The compounds B_4X_4 are therefore of interest. Gas-phase electron diffraction investigations (possible without using any computed data to assist the refinements) of tetra-*tert*-butyltetrabora-tetrahedrane, $B_4(t\text{-Bu})_4$, **15** (Figure 15),[D28] has been carried out under the condition of T symmetry. The high symmetry of this system has ensured the quality of experimental geometry determined by GED alone (the sample was provided by the University of Aachen and data recorded in Oslo). In particular, torsional angles in **15** have been determined accurately on the basis of a very small time scale of this method, including τ(B–B–C–C) = 30.3(3)°. Interestingly, the B atom is extremely deshielded, with δ(^{11}B) 135.4 ppm. This value is satisfactorily reproduced computationally only by taking dynamic electron correlation into account, then yielding chemical shift of 139 ppm with the GIAO-MP2/TZP′ method.

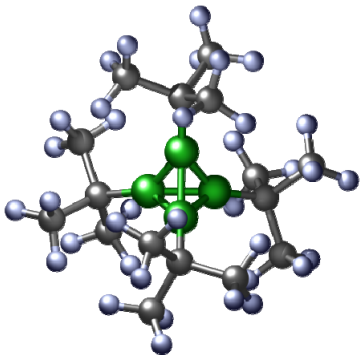

Fig. 15 Tetra-*tert*-butyltetraboratetetrahedrane

6. Shared icosahedra

As well as main-group elements that can be incorporated into boron frameworks, it is also possible to have metal atoms as parts of such clusters, known as metallaheteroboranes. There is a plethora of such deltahedral compounds, most prominent among them being the so-

called *commo*-bis(icosahedral)metallacarbaboranes of the type $[M(1,2\text{-}C_2B_9H_{11})_2]^{n-1}$, in which two icosahedra are conjoined by a shared metal-atom vertex. The most investigated and best known is the anionic $[3\text{-}Co\text{-}(1,2\text{-}C_2B_9H_{11})_2]^-$, usually referred to as the cobalt bis(dicarbollide) ion. Two dicarbollide anions are complexed with Ni^{4+} to give a neutral sandwich system. A DFT study at the BP86/AE1 level[D29] (**16**, Figure 16) has found that the mutual rotation of the two dicarbollide moieties is facile. Note that such a molecular shape is based on sharing two icosahedra through one vertex (Ni^{4+}). Experimental ^{11}B NMR chemical shifts are reproduced to better than 3 ppm at the GIAO-B3LYP/II′ level. The same DFT approach has been employed for other heteroboranes in this study but none of them is neutral. The nickel sandwich **16** appears to act as a molecular rotor.[33]

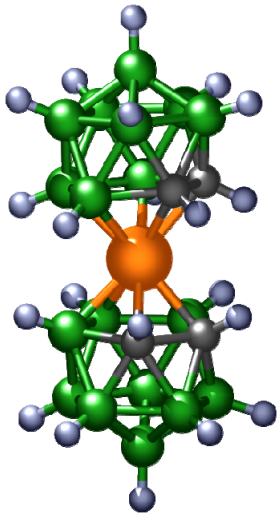

Fig. 16 The most stable rotamer of $[3\text{-}Ni(1,2\text{-}C_2B_9H_{11})_2]$

In a similar way to two benzene rings fusing to form naphthalene, the combination of two of *closo*-$B_{12}H_{12}^{2-}$ forms so-called macropolyhedral clusters (other parent boron hydrides can also be shared), the molecular geometries of which depend on the mode of sharing. Apart from the aforementioned one-vertex sharing, there are other modes of two-icosahedra sharing. They can also be joined through a common edge or three or four vertices come together. The latter is exemplified in macropolyhedral $B_{20}H_{16}$, the first synthesised *closo* macropolyhedron.[34] Indeed, the latter has four joint vertices of two shared icosahedra *closo*-$B_{12}H_{12}^{2-}$, **17** (Figure 17). This unique cluster was obtained relatively recently in another way

and was structurally characterised in terms of applying the GIAO-B3LYP/II//MP2/6-31G* computational protocol.[D30]

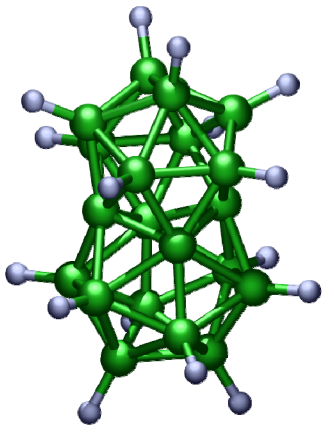

Fig. 17 Macropolyhedral cluster, $B_{20}H_{16}$

B GALLIUM CLUSTERS

Some neutral boron hydrides of larger dimensions (e.g very well known $B_{18}H_{22}$) are used as boron-dopant agents in microelectronics. It is not aluminium but gallium that is also used in this field, mainly in the form of cluster-like gallium nitride. On that basis, structural examination of other gallium clusters using GED was challenging.

Although boron and gallium belong to the same group of elements, their structural chemistries differ significantly. In contrast to boron, gallium does not form electron deficient clusters to such a large extent, although examples do exist. One example is digallane, Ga_2H_6, whose structure was determined by electron diffraction with the same D_{2h} model as interpreted for diborane.[35] Apart from this boron-type compound, Ga in the form of GaH or GaH_2 moieties can be incorporated into polyborane or carborane clusters as exemplified by $H_2GaB_3H_8$, successfully explored using electron diffraction.[36] The anionic $[3\text{-Ga-}(1,2\text{-}C_2B_9H_{11})_2]^-$ bears a strong resemblance to **16** and other metallaboranes of this type.[37] Interestingly, there are gallium clusters that have a similar structural motif to **15**. They are present in the distorted cubane cores of Ga_4E_4 (E = S,[D31] **18a**, Se,[D32] **18b**) and the corresponding samples were provided by Harvard University, Cambridge, USA. Both cubanes are present in the form $[(t\text{-Bu})GaE]_4$ with bulky *tert*-butyl groups bonded to gallium atoms. The electron diffraction analyses took models with *T* symmetries into account. Indeed,

the heavy-atom skeletons can be considered as two penetrating tetrahedra, *viz.* Ga_4 and E_4. The cubane-like structures are based on the distortion of regular cubic geometries, which is reflected by the Ga–E–Ga angles narrower than 90° and the E–Ga–E angles wider than 90°. As a consequence, each face on the polyhedron is rhombic with a fold on the diagonal Ga···Ga (*ca.* 10°). This is clearly significant given that the majority of dimeric gallium compounds are planar. Both VSEPR theory and Jahn-Teller distortion offer possible explanations for this observation. The decomposition of these cubanes, namely the metal-organic chemical vapour deposition (MOCVD), result in growing new phases of GaE.[D31,D32]

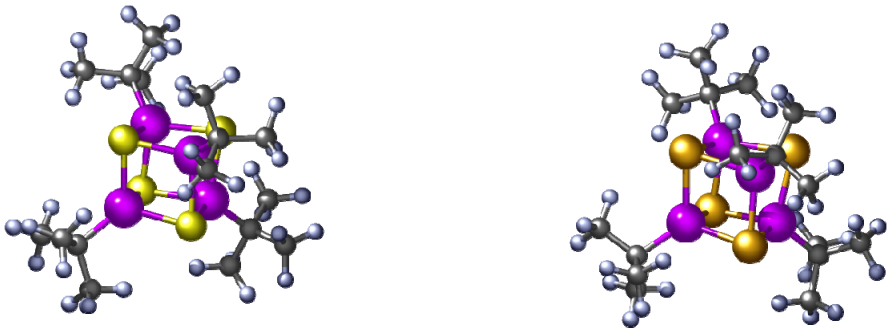

18a **18b**

Fig. 18 Perspective views of the both $[(t\text{-Bu})GaE]_4$

CONCLUSIONS AND OUTLOOK

This thesis has illustrated the use of structural information to better understand various series of neutral borane and heteroborane clusters, which were prepared in Řež and elsewhere, and structurally characterised in Edinburgh and/or Řež. Two gallium clusters were also studied. The results are summarized in Table 1.

Table 1 Boron and gallium clusters structurally studied

	Method		
	MOCED[a]	SARACEN[b]	QCH[c]
Cluster type	Molecule (point group of symmetry)		
closo	1-$NB_{11}H_{12}$ (C_{5v}) 1,2-$C_2B_8H_{10}$ (C_s) 1-$SB_{11}H_{11}$[d, e] (C_{5v}) 1,7-Cl_2-1,7-$C_2B_{10}H_{10}$ (C_{2v}) 1,12-$(SH)_2$-1,12-$C_2B_{10}H_{10}$[f] (C_2)	1-$SeB_{11}H_{11}$ (C_{5v}) 1-SB_9H_9[d] (C_{4v}) 1-ph-1,2-$C_2B_{10}H_{11}$[e] (C_1) 9,12-$(SH)_2$-1,2-$C_2B_{10}H_{10}$ (C_1)	1,2-$P_2B_{10}H_{10}$ (C_{2v}) 1,7-$P_2B_{10}H_{10}$ (C_{2v}) 2,1-PCB_8H_9 (C_s) 6,1-PCB_8H_9 (C_s) 12-F-1-$SB_{11}H_{10}$ (C_{5v}) 12-Cl-1-$SB_{11}H_{10}$[e] (C_{5v}) 12-Br-1-$SB_{11}H_{10}$[e] (C_{5v}) 12-I-1-$SB_{11}H_{10}$[e] (C_{5v})
nido	7,8,10-$C_2SB_8H_{10}$ (C_s)		7,8,9,11-$P_2C_2B_7H_9$ (C_s) 7,9,8,10-$P_2C_2B_7H_9$ (C_1) 7,8,9,10-$P_2C_2B_7H_9$ (C_1)
arachno	B_5H_{11} (C_1) B_6H_{12} (C_2)	6,9-$C_2B_8H_{14}$ (C_{2v}) 6,9-CSB_8H_{12} (C_s) 4,6-$C_2B_7H_{13}$ (C_s) 4,6-$S_2B_7H_9$ (C_s)	6,9-$N_2B_8H_{12}$ (C_{2v}) 6,9-$Se_2B_8H_{10}$ (C_{2v}) 6,9-CNB_8H_{13} (C_s) 4,6,5-$C_2SB_6H_{10}$ (C_s)
X_4 (X=B, Ga)	2,4-$CH_2CH_2B_4H_8$ (C_{2v}) 2,4-(*t*-$BuCHCH_2$)B_4H_8 (C_2) B_4(*t*-Bu)$_4$[g] (T) [GaS]$_4$(*t*-Bu)$_4$[g,h] (T) [GaSe]$_4$(*t*-Bu)$_4$[g,h] (T)		
Shared icosahedra			$B_{20}H_{16}$ (D_{2d}) [3-Ni(1,2-$C_2B_9H_{11}$)$_2$] (C_1)

[a]Computed constraints fixed during electron diffraction refinements, computations of ^{11}B chemical shift performed.

[b]Computed restraints fixed during electron diffraction refinements, computations of ^{11}B chemical shift performed.

[c]Quantum-chemical calculations using the ab initio/IGLO/NMR approach with DFT and GIAO variants.

[d]MW structures also determined.

[e]Experimental dipole moments measured and interpreted.

[f]A series of mono- and disubstituted derivatives of 1,12-$C_2B_{10}H_{12}$ prepared for the purpose of electric dipole moment measurements and their interpretation.

[g]GED alone, only some angular parameters (either vibrational amplitudes or valence angles) fixed.

[h]Two Ga_4 tetrahedra mutually fused.

Much of what is described involved the application of gas-phase electron diffraction and calculations of ^{11}B NMR chemical shifts (used as an additional electron-diffraction refinement condition) to yield molecular geometries of various species that were validated against experimental NMR data. Such gas-phase (and computed) structures are of particular significance since the free molecules can be considered unperturbed and the resulting macro-structure is influenced exclusively by intramolecular forces. The systems that contain a heavy element (through hydrogen or vertex substitution) are suitable targets for structural studies employing GED alone and the corresponding results may thus verify the reliability of theoretical approaches. The gas-phase structures under scrutiny turned out to be quite rigid in terms of the vibrational amplitudes obtained. This observation is particularly true for *closo* clusters. They have electron density distributions that are counterintuitive to the concept of electronegativity as also revealed by the analyses of the experimental dipole moments. (Indeed, carbon is more electronegative than boron but its charge is positive, and the same applies to sulfur.) In addition to the structural studies that have been, and will be, performed for the series of boron clusters described, there is great potential for study of the macropolyhedral clusters (see Fig. 17). Some of these have been known for decades, but accurate structural studies of them are entirely lacking. They are therefore a challenging target for applications both of GED and computational protocols in this demanding but important area of boron cluster chemistry.

On the basis of electron distribution in 12-Ph-*closo*-1-$SB_{11}H_{10}$, a new type of nonclassical σ-hole-based noncovalent interaction, the chalcogen bonding, has been very

recently discovered, which offers a promising use for *closo*-heteroboranes with V and VI group elements in crystal engineering and drug design.[38] There are other areas where the use of boron clusters in medicine, molecular electronics and materials science also looks promising. Whereas some metallaboranes appear to be potent inhibitors of various enzymes and to act as molecular rotors, some thiolated carbaboranes act as modifiers of layers of various metals.[39] In this context, the synthetic efforts aimed at development of further *closo*-, *nido*- *arachno*- and macropolyhedral clusters along with the subsequent molecular structure determinations is obvious. Note that neutral macropolyhedral boranes (such as $B_{20}H_{16}$) represent challenging materials as boron-dopant agents in the fabrication of p-type semiconducting silicon.

Similarly, the role of gallium in microelectronics as well as in materials science is quite apparent and, consequently, there is demand for structures containing gallium to help interpret the properties of such clusters.

Generally speaking, the joint endeavour of studying synthesis and structure in a concerted manner is worth striving for because "*there is no more basic enterprise in chemistry than the determination of the geometrical structure of a molecule. Such a determination, when it is well done, ends all speculation as to the structure and provide us with starting point for the understanding of every physical, chemical and biological property of the molecule*", Roald Hoffmann, Nobel Prize Winner in Chemistry (1981).[40]

October 29, 2014

PUBLICATIONS THAT FORM THE BASIS OF THE THESIS

D1. This approach was first introduced in the structure analysis for *closo*-1-$NB_{11}H_{12}$: D. Hnyk, M. Bühl, P. v. R. Schleyer, H. V. Volden, S. Gundersen, J. Müller and P. Paetzold, *Inorg. Chem.*, 1993, **32**, 2442.

D2. P. T. Brain, D. Hnyk, D. W. H. Rankin, M. Bühl and P. v. R. Schleyer, *Polyhedron*, 1994, **13**, 1453.

D3. D. Hnyk, E. Vajda, M. Bühl and P. v. R. Schleyer, *Inorg. Chem.*, 1992, **31**, 2464.

D4. H. Møllendal, S. Samdal, J. Holub and D. Hnyk, *Inorg. Chem.*, 2003, **42**, 3043.

D5. J. Macháček, J. Plešek, J. Holub, D. Hnyk, V. Všetečka, I. Císařová, M. Kaupp and B. Štíbr, *Dalton Trans.*, 2006, 1024.

D6. S. Heřmánek, D. Hnyk and Z. Havlas, *J. Chem. Soc., Chem. Commun.*, 1989, 1859;

D7 M. Bühl, P. v. R. Schleyer, Z. Havlas, D. Hnyk and S. Heřmánek, *Inorg. Chem.*, 1991, **30**, 3107.

D8. D. Hnyk, D. A. Wann, J. Holub, M. Bühl, H. E. Robertson and D. W. H. Rankin, *Dalton Trans.*, 2008, 96.

D9. P. T. Brain, J. Covie, D. J. Donohoe, D. Hnyk, D. W. H. Rankin, D. Reed, B. D. Reid, Robertson, H.E. , Welch, A.J., Hofmann, M. and Schleyer, P.v.R.: *Inorg. Chem.*, 1996, **35**, 1701

D10. D. A. Wann, P. D. Lane, H. E. Robertson, T. Baše and D. Hnyk, *Dalton Trans.* 2013, **42**, 12015.

D11. D. Hnyk, P. T. Brain, H. E. Robertson, D. W. H. Rankin, M. Hofmann, P. v. R. Schleyer and M. Bühl, *J. Chem. Soc., Dalton Trans.*, 1994, 2885.

D12. D. Hnyk, J. Holub, M. Hofmann, P. v. R. Schleyer, H. E. Robertson and D. W. H. Rankin, *J. Chem. Soc., Dalton Trans.*, 2000, 4617.

D13. D. Hnyk, V. Všetečka, L. Drož and O. Exner, *Collect. Czech. Chem. Commun.*, 2001, **66**, 1375.

D14. L. Drož, M. A. Fox, D. Hnyk, P. J. Low, J. A. H. MacBride and V. Všetečka, *Collect. Czech. Chem. Commun.*, 2009, **74**, 131.

D15. B. Grüner, D. Hnyk, I. Císařová, Z. Plzák and B. Štíbr, *J. Chem. Soc., Dalton Trans.*, 2002, 2954.

D16. H. Møllendal, S. Samdal, J. Holub and D. Hnyk, *Inorg. Chem.*, 2002, **41**, 4574.

D17. D. Hnyk, D. A. Wann, J. Holub, S. Samdal and D. W. H. Rankin, *Dalton Trans.*, 2011, **40**, 5734.

D18. D. Hnyk, D. W. H. Rankin, H. E. Robertson, M. Hofmann, P. v. R. Schleyer and M. Bühl, *Inorg. Chem.*, 1994, **33**, 4781.

D19. J. Holub, M. Bakardjiev, B. Štíbr, D. Hnyk, O. L. Tok and B. Wrackmeyer, *Inorg. Chem.*, 2002, **41**, 2817.

D20. D. Hnyk, M. Hofmann, P. v. R. Schleyer, M. Bühl and D. W. H. Rankin, *J. Phys. Chem.*, 1996, **100**, 3435.

D21. J. Holub, T. Jelínek, D. Hnyk, Z. Plzák, I. Císařová, M. Bakardjiev and B. Štíbr, *Chem. Eur. J.*, 2001, **7**, 1546.

D22. D. Hnyk, M. Bühl, J. Holub, S. A. Hayes, D. A. Wann, I. D. Mackie, K. B. Borisenko, H. E. Robertson and D. W. H. Rankin, *Inorg. Chem.*, 2006, **45**, 6014.

D23. D. Hnyk, J. Holub, S. A. Hayes, M. F. Robinson, D. A. Wann, H. E. Robertson and D. W. H. Rankin, *Inorg. Chem.*, 2006, **45**, 8442.

D24. D. A. Wann, P. D. Lane, H.E. Robertson, J. Holub and D. Hnyk, *Inorg. Chem.*, 2013, **52**, 4502.

D25. D. Hnyk, M. Hofmann and P. v. R. Schleyer, *Collect. Czech. Chem. Commun.*, 1999, **64**, 993.

D26. The compound is formally classified as a *hypho*-dicarbaborane ($4n + 8 = 32$ valence electrons) but it is more usual to regard it as an ethene adduct of tetraborane(8): D. Hnyk, P. T. Brain, D. W. H. Rankin, H. E. Robertson, R. Greatrex, N. N. Greenwood, M. Kirk, M. Bühl and P. v. R. Schleyer, *Inorg. Chem.*, 1994, **33**, 2572.

D27. P. T. Brain, M. Bühl, M. A. Fox, R. Greatrex, D. Hnyk, A. Nikrahi, D. W. H. Rankin and H. E. Robertson, *J. Mol. Struct.*, 1998, **445**, 319.

D28. D. Hnyk, *Polyhedron*, 1997, **16**, 603.

D29. M. Bühl, J. Holub, D. Hnyk and J. Macháček, *Organometallics*, 2006, **25**, 2173.

D30. D. Hnyk, J. Holub, T. Jelínek, J. Macháček and M. G. S. Londesborough, *Collect. Czech. Chem. Commun.*, 2010, **75**, 1115.

D31. W. M. Cleaver, M. Späth, D. Hnyk, G. McMurdo, M. B. Power, M. Stuke, D. W. H. Rankin and A. R. Barron, *Organometallics*, 1995, **14**, 690.

D32. M. B. Power, A. R. Barron, D. Hnyk, H. E. Robertson and D. W. H. Rankin, *Adv. Mater. Opt. Electr.*, 1995, **5**, 177.

Publication report

Number of all papers: **93**
Sum of the Times Cited: **1068**
Sum of the Times Cited without self-citations: **794**
ResearcherID: **F-9043-2014**
h-index: **19**

REFERENCES

1. S. H. Bauer, *J. Am. Chem. Soc.*, 1937, **59**, 1096.
2. K. Hedberg and V. Schomaker, *J. Am. Chem. Soc.*, 1951, **73**, 1482.
3. B. Štíbr, *Chem. Rev.*, 1992, **2**, 225; J. Plešek, *Chem. Rev.*, 1992, **2**, 269; S. Heřmánek, *Chem. Rev.*, 1992, **2**, 325. The first IMEBORON (International Meeting on Boron Chemistry) was held in the former Czechoslovakia, Liblice Castle, 1971. This was repeated in 1987 at Bechyně Castle. The 3rd EUROBORON (European Meeting on Boron Chemistry) was held in the Czech Republic, Průhonice-by-Prague, 2004. The 15th IMEBORON was held in Prague in August 2014.
4. Microwave spectroscopy is also of some importance, but only for molecules with permanent dipole moments; the large number of $^{10}B/^{11}B$ isotopomers can cause problems.
5. I. Hargittai, In: I. Hargittai and M. Hargittai (Eds.), Stereochemical Applications of Gas-Phase Electron Diffraction, VCH Publishers, Weinheim and New York, 1988, Part A.
6. For example, the molecule (COD)Cu(hfac) is quite tricky to model: D. Hnyk, M. Bühl, P. T. Brain, H. E. Robertson and D. W. H. Rankin, *J. Am. Chem. Soc.*, 2002, **124**, 8078. The same applies to, for example, CEt_4: R. W. Alder, P. R. Allen, D. Hnyk, D. W. H. Rankin, H. E. Robertson, B. A. Smart, R. J. Gillespie and I. Bytheway, *J. Org. Chem.*, 1999, **64**, 4226. In contrast, just one and two parameters are needed to model CO and H_2O, respectively.
7. V. J. Klimkowski, J. D. Ewbank, C. van Alsenoy and L. Schäfer, *J. Am. Chem. Soc.*, 1982, **104**, 1476.
8. A. J. Blake, P. T. Brain, H. McNab, J. Miller, C. A. Morrison, S. Parsons, D. W. H. Rankin, H. E. Robertson and B. A. Smart, *J. Phys. Chem.*, 1996, **100**, 12280; N. W. Mitzel and D.W.H. Rankin, *Dalton Trans.*, 2003, 3650.
9. Individual Gauge for Localised Orbitals: W. Kutzelnigg, U. Fleischer and M. Schindler, in: NMR Basic Principles and Progress, Springer-Verlag, Berlin Heidelberg, 1990, vol. 23, 165.
10. Gauge-Including Atomic Orbitals: R. Ditchfield, *Mol. Phys.*, 1974, **27**, 789.
11. J. S. Binkley and J. A. Pople, *Int. J. Quantum Chem.*, 1975, **9**, 22 and references cited therein.

12. S. Huzinaga, Approximate Atomic Wave Functions, University of Alberta, Edmonton, Canada, 1971.
13. W. Hehre, L. Radom, P. v. R. Schleyer and J. A. Pople, ab Initio Molecular Orbital Theory, Wiley, New York, 1986.
14. A. D. Becke, *J. Chem. Phys.*, 1993, **98**, 5648; C. Lee, W. Yang and R. G. Parr, *Phys. Rev. B*, 1988, **37**, 785.
15. A. D. Becke, *Phys. Rev. A*, 1988, **38**, 3098; J. P. Perdew, *Phys. Rev. B*, 1986, **33**, 8822.
16. See, for example, M. Schindler, *J. Am. Chem. Soc.*, 1987, **109**, 1020.
17. R. A. Beaudet, In: J. F. Liebmann, A. Greenberg and R. E. Williams (Eds.), Advances in Boron and the Boranes, VCH Publishers, New York, 1988, Chapter 20, 417.
18. M. Bühl and P. v. R. Schleyer, *J. Am. Chem. Soc.*, 1992, **114**, 477.
19. V. S. Mastryukov, in: I. Hargittai and M. Hargittai (Eds.), Stereochemical Applications of Gas-Phase Electron Diffraction, VCH Publishers, Weinheim and New York, 1988, Part B.
20. P. v. R. Schleyer, M. Bühl, U. Fleischer and W. Koch, *Inorg. Chem.*,1990, **29**, 153.
21. R. Greatrex, N. N. Greenwood, D. W. H. Rankin and H. E. Robertson, *Polyhedron*, 1987, **6**, 1849.
22. R. Greatrex, N. N. Greenwood, M. B. Millikan, D. W. H. Rankin and H. E. Robertson, *J. Chem. Soc., Dalton Trans.*, 1988, 2335.
23. M. Bühl and P. v. R. Schleyer, *Angew. Chem., Int. Ed.*, 1990, **29**, 153.
24. R. Zahradník, V. Balaji and J. Michl, *J. Comput. Chem.*, 1991, **12**, 1147.
25. W. J. Hehre, R. Ditchfield and J. A. Pople, *J. Chem. Phys.*, 1972, **56**, 2257.
26. For BI_4^- and BI_3 the spin-orbit corrections are predominant in terms of reproducing experimental values, D. Hnyk and J. Macháček, XIIth International Congress of Quantum Chemistry, Kyoto, Japan, May 21-26, 2006.
27. S. Korbe, P. J. Schreiber and J. Michl, *Chem. Rev.*, 2006, **106**, 5208.
28. Indeed, Bohn and Bohn carried out such investigations but only the structure of **4c** was determined accurately, R. K. Bohn and M. D. Bohn, *Inorg. Chem.*, 1971, **10**, 350; precise structures based on *SARACEN* are in A. R. Turner, H. E. Robertson, K. B. Borisenko, D. W. H. Rankin and M. A. Fox, *Dalton Trans.*, 2005, 1310. Due to the zero dipole moment of **4c**, microwave spectroscopy was applied only to **4a** and **4b**, see: S. Samdal, H. Møllendal, D. Hnyk and J. Holub, *J. Phys. Chem. A*, 2011, **115**, 3380.

29. A. Domenicano, In: I. Hargittai and M. Hargittai (Eds.), Stereochemical Applications of Gas-Phase Electron Diffraction, VCH Publishers, Weinheim and New York, 1988, Part B.
30. Computed details of other (*closo*-$CB_nH_{n+1})^-$ systems are given in P.v.R. Schleyer and K. Najafian, *Inorg. Chem.*, 1998, **37**, 3454; some of them were just predicted, *e.g.* $CB_6H_7^-$ and $CB_8H_9^-$. The latter were eventually prepared and structurally characterised by the GIAO-MP2/II//MP2/6-31G* method; $CB_6H_7^-$: B. Štíbr, *Angew. Chem., Int. Ed.*, 2002, **41**, 2126; $CB_8H_9^-$: T. Jelínek, *Chem. Commun.*, 2001, 1756.
31. E. G. Atavin, V. S. Mastryukov, A. V. Golubinskii and L. V. Vilkov, *J. Mol. Struct.*, 1980, **65**, 259.
32. K. Wade, *Adv. Inorg. Chem. Radiochem.*, 1976, **18**, 1.
33. M. F. Hawthorne, J. I. Zink, J. M. Skeleton, M. J. Bayer, Ch. Liu, E. Livshits, R. Baer and D. Neuhauser, *Science*, 2004, **303**, 1849. Similarly, protonated and deprotonated [3-Fe-(1,2-$C_2B_9H_{11})_2H$] also appears as molecular rotor: M. Bühl, D. Hnyk and J. Macháček, *Inorg. Chem.*, 2007, **46**, 1771.
34. N. E. Miller and E. L. Muetterties, *J. Am. Chem. Soc.*, 1963, **85**, 3506.
35. A. J. Downs, T. M. Greene, E. Johnsen, C. R. Pulham, H. E. Robertson and D. A. Wann, *Dalton Trans*., 2010, **39**, 5637.
36. C. R. Pulham, A. J. Downs, D. W. H. Rankin and H. E. Robertson, *J. Chem. Soc., Dalton Trans.*, 1992, 1509.
37. M. A. Bandman, C. B. Knobler and M. F. Hawthorne, *Inorg. Chem.*, 1989, **28**, 1206.
38. J. Fanfrlík, A. Přáda, Z. Padělková, A. Pecina, J. Macháček, M. Lepšík, J. Holub, A. Růžička, D. Hnyk and P. Hobza, *Angew. Chem.*, *Int. Ed.*, 2014, 2014, **53,** 10139 – 10142.
39. Inhibition of HIV protease: P. Cígler, M. Kožíšek, P. Řezáčová, J. Brynda, Z. Otwinowski, J. Pokorná, J. Plešek, B. Grüner, L. Dolečková-Marešová, M. Máša *et al*., *Proc. Natl. Acad. Sci. USA*, 2005, **102**, 15394; inhibition of carbonic anhydrase: J. Brynda, P. Mader, V. Šícha, M. Fábry, K. Poncová, M. Bakardiev, B. Grüner, P. Cígler and P. Řezáčová, *Angew. Chem. Int. Ed.*, 2013, **52**, 13760; modifications of gold layers: T: Baše, Z. Bastl, Z. Plzák, T. Grygar, J. Plešek, V. Malina, J. Šubrt, J. Boháček, E. Večerníková and O. Kříž, *Langmuir*, 2005, **21**, 7776.

40. R. Hoffmann, in Foreword of L. V. Vilkov, V. S. Mastryukov and N. I. Sadova, Determination of the Geometrical Structure of Free Molecules, Mir Publishers, Moscow, 1983.